To appear in the *International Journal of Systems Science*
Vol. 00, No. 00, Month 20XX, 1–22

Set-Membership Parity Space Hybrid System Diagnosis

Jorge Vento[†] , Joaquim Blesa[*,1], Vicenç Puig[*,1] and Ramon Sarrate[†]

[†]*Automatic Control Department, Universitat Politècnica de Catalunya (UPC), Rambla de Sant Nebridi, 11, 08222 Terrassa, Spain*

[*,1] *Institut de Robòtica i Informàtica Industrial (CSIC-UPC), Llorens i Artigas, 4-6, 08028 Barcelona, Spain*

(*Received 00 Month 20XX; final version received 00 Month 20XX*)

In this paper, diagnosis for hybrid systems using a parity space approach that considers model uncertainty is proposed. The hybrid diagnoser is composed of modules which carry out the mode recognition and diagnosis tasks interacting each other, since the diagnosis module adapts accordingly to the current hybrid system mode. Moreover, the methodology takes into account the unknown but bounded uncertainty in parameters and additive errors using a passive robust strategy based on the set-membership approach. An adaptive threshold that bounds the effect of model uncertainty in residuals is generated for residual evaluation using zonotopes, and the parity space approach is used to design a set of residuals for each mode. The proposed fault diagnosis approach for hybrid systems is illustrated on a piece of the Barcelona sewer network.

Keywords: Fault detection and isolation, hybrid systems, parameter uncertainty, mode recognition , diagnoser.

1. Introduction

Most real systems are on-line controlled and supervised by means of automatic computer-based control systems. But, they are subject to faults that can appear in the plant components, sensors and actuators. Many of these systems present a behavior that changes with the operating mode, where every mode corresponds to a discrete-state of the system that could have a different behaviour (i.e., continuous dynamic model). These systems are better described using hybrid models that integrate continuous and discrete dynamics. There are several hybrid modelling approaches as, e.g. hybrid automaton models (Hofbaur and Williams 2004) or hybrid bond graph models (Narasimhan and Biswas 2007; Daigle 2008). Hybrid models can be used for the system monitoring, fault diagnosis and control tasks. Model-based online diagnosis requires quick and robust reconfiguration processes when a mode change occurs, as well as the ability to keep the nominal behavior of the system on track during transient states (Bregon et al. 2010). On-line fault diagnosis allows reconfiguring the system after the fault appearance, by activating some fault tolerance mechanisms, increasing the system resilience (i.e., the capability to recover the system functions after a partial system damage has occurred)(Blanke et al. 2006).

Recently, in the literature, model based techniques have been proposed to diagnose hybrid systems (Travé-Massuyès et al. 2008; Cocquempot et al. 2004; Daigle 2008). The continuous behavior in each mode is described using differential equations. These techniques extend, in some way, existing model-based approaches for non-hybrid systems being able to handle the continuous and discrete-event system behaviors. In a hybrid system, the diagnoser should be parameterized as a function of the current mode. Thus, the proposed diagnoser should be able to evaluate the behavior of the hybrid system online, and to detect and isolate the mode and the faults. In Travé-Massuyès et al. (2008), the discrete-event behavior

[†]Corresponding author. e-mail: jorge.isaac.vento@upc.edu

is modeled as a set of discrete modes, that can include nominal or faulty modes, and transitions between them are governed by events. Following the methodology proposed by Sampath et al. (1995) and Vento et al. (2011), a diagnoser combining the discrete and the continuous dynamics is built by means of a behavior automaton. In Cocquempot et al. (2004), a global vision on how to detect and isolate faults in hybrid systems by generating the set of residuals is provided. However, a formal methodology to build a hybrid diagnoser is not proposed, and measurement uncertainty is not accounted for.

The contribution of this paper is to present a fault diagnosis method for hybrid systems where the current operation mode is recognized by generating a set of residuals designed by means of the parity space approach and that taking into account model uncertainty in the residual evaluation. The robustness is enhanced using a passive strategy based on generating an adaptive threshold that considers the effect of parameter and additive error uncertainty (including noise and discretization errors) in the residual evaluation using zonotopes, extending the results presented in Blesa et al. (2012); Vento et al. (2012) to hybrid systems.

The structure of this paper is the following. In Section 2, the hybrid model is defined, which accounts for parameter uncertainty. In Section 3, the fault detection technique for hybrid systems is introduced. Fault isolation and mode recognition are described in Section 4 and Section 5, respectively. In Section 6, an application case study based on the sewer network of the Barcelona city is used to assess the validity of the proposed approach. Finally, Section 7 summarizes the main paper conclusions.

2. Problem Statement

2.1 *Hybrid model*

Let us consider that the model of the hybrid system to be diagnosed can be described by the following hybrid automaton $HA =< \mathcal{Q}, \mathcal{X}, \mathcal{U}, \mathcal{Y}, \mathcal{F}, \mathcal{G}, \mathcal{H}, \Sigma, \mathcal{T} >$, where:

- $\mathcal{Q}$ is a set of modes. Each $q_i \in \mathcal{Q}$ represents a nominal operation or a faulty mode of the system i.e. $\mathcal{Q} = \mathcal{Q}_{\mathcal{N}} \cup \mathcal{Q}_{\mathcal{F}}$ with $|\mathcal{Q}| = n_q$.
- $q_0 \in \mathcal{Q}$ is the initial mode.
- $\mathcal{X} \subseteq \Re^{nx}$ defines the discrete-time continuous state space. $\mathbf{x}(k) \in \mathcal{X}$ is the discrete-time state vector at sample k and $\mathbf{x}_0$ the initial state vector.
- $\mathcal{U} \in \Re^{nu}$ defines the discrete-time continuous input space. $\mathbf{u}(k) \in \mathcal{U}$ is the discrete-time continuous input vector.
- $\mathcal{Y} \in \Re^{ny}$ defines the discrete-time continuous output space. $\mathbf{y}(k) \in \mathcal{Y}$ is the discrete-time continuous output vector.
- $\mathcal{F}$ is a set of faults. Every faulty mode $q_i \in Q_{\mathcal{F}}$ corresponds to a fault $f_i \in \mathcal{F}$ as well as a fault event $\sigma_f \in \Sigma_{\mathcal{F}}$.
- $\mathcal{G}$ defines a set of discrete-time state affine functions with parametric uncertainty for each nominal mode [1]:

$$\mathbf{x}(k+1) = \mathbf{A}_i(\widetilde{\boldsymbol{\theta}})\mathbf{x}(k) + \mathbf{B}_i(\widetilde{\boldsymbol{\theta}})\mathbf{u}(k) + \mathbf{F}_{xi}(\widetilde{\boldsymbol{\theta}})\mathbf{f}(k) + \mathbf{E}_{xi}(\widetilde{\boldsymbol{\theta}}) \tag{1}$$

  where $\mathbf{A}_i(\widetilde{\boldsymbol{\theta}}) \in \Re^{nx \times nx}$, $\mathbf{B}_i(\widetilde{\boldsymbol{\theta}}) \in \Re^{nx \times nu}$ and $\mathbf{E}_{xi}(\widetilde{\boldsymbol{\theta}}) \in \Re^{nx \times 1}$ are the state matrices in mode i, and $\mathbf{f}(k) \in \Re^{nf}$ represents the system faults, with $\mathbf{F}_{xi}(\widetilde{\boldsymbol{\theta}}) \in \Re^{nx \times nf}$ being the fault distribution matrix in mode i. The model parameters $(\widetilde{\boldsymbol{\theta}})$ are considered unknown but bounded by an interval set, i.e., they belong to the set $\boldsymbol{\Theta} = \{\boldsymbol{\theta} \in \Re^{n\boldsymbol{\theta}} | \underline{\boldsymbol{\theta}} \leq \boldsymbol{\theta} \leq \overline{\boldsymbol{\theta}}\}$. This set represents the uncertainty on the exact knowledge of the real system parameters $(\widetilde{\boldsymbol{\theta}})$.
- $\mathcal{H}$ defines a set of discrete-time output affine functions with parametric uncertainty for each nom-

[1] The effect of the fault is assumed unknown and modeled by the vector **f**.

inal mode [1]:

$$\mathbf{y}(k) = \mathbf{C}_i(\widetilde{\boldsymbol{\theta}})\mathbf{x}(k) + \mathbf{D}_i(\widetilde{\boldsymbol{\theta}})\mathbf{u}(k) + \mathbf{F}_{y_i}(\widetilde{\boldsymbol{\theta}})\mathbf{f}(k) + \mathbf{E}_{y_i}(\widetilde{\boldsymbol{\theta}}) + \mathbf{N}_i\widetilde{\mathbf{n}}(k) \tag{2}$$

where $\mathbf{C}_i(\widetilde{\boldsymbol{\theta}}) \in \Re^{ny\times nx}$, $\mathbf{D}_i(\widetilde{\boldsymbol{\theta}}) \in \Re^{ny\times nu}$ and $\mathbf{E}_{y_i}(\widetilde{\boldsymbol{\theta}}) \in \Re^{ny\times 1}$ are the output matrices in mode i and $\mathbf{F}_{y_i}(\widetilde{\boldsymbol{\theta}}) \in \Re^{ny\times nf}$ is the fault distribution matrix in mode i. $\widetilde{\mathbf{n}}(k) \in \mathcal{V}$ is a vector of dimension $n_{\widetilde{\mathbf{n}}} \times 1$ corresponding to the additive error that includes the effects of noise in measurements and discretisation errors. The additive error is unknown but it is assumed to be bounded by a set $\mathcal{V}$.

- $\Sigma = \Sigma_s \cup \Sigma_c \cup \Sigma_f$ is a set of events. Spontaneous mode switching events (Σ_s), input events (Σ_c) and fault events Σ_f are considered. Each spontaneous event $\sigma_s \subseteq \Sigma_s$ defines when the state vector intersects a jump surface $S_{\sigma_s} = \{\mathbf{x}(k) \in \mathcal{X} : s_{\sigma_s}(\mathbf{x}(k)) = \mathbf{0}\}$, with s_{σ_s} being a linear switching condition. Σ can be partitioned into $\Sigma_o \cup \Sigma_{uo}$ where Σ_o represents the set of observable events and Σ_{uo} represents the set of unobservable events. It is assumed that $\Sigma_f \subseteq \Sigma_{uo}$, $\Sigma_c \subseteq \Sigma_o$ and Σ_s can be contained in both partitions.
- $\mathcal{T} : \mathcal{Q} \times \Sigma \to \mathcal{Q}$ defines a partial discrete state transition function.

Alternatively, the model given by (1)-(2) can be expressed in input-output form using the shift p-operator (or delay operator) assuming zero initial conditions as follows

$$\mathbf{y}(k) = \mathbf{M}_i(p^{-1}, \widetilde{\boldsymbol{\theta}})\mathbf{u}(k) + \boldsymbol{\Upsilon}_i(p^{-1}, \widetilde{\boldsymbol{\theta}})\mathbf{f}(k) + \mathbf{E}_{mi}(p^{-1}, \widetilde{\boldsymbol{\theta}}) + \boldsymbol{\Omega}_i(p^{-1})\widetilde{\mathbf{n}}(k) \tag{3}$$

where:

$$\begin{aligned}
\mathbf{M}_i(p^{-1}, \widetilde{\boldsymbol{\theta}}) &= \mathbf{C}_i(\widetilde{\boldsymbol{\theta}})(p\mathbf{I} - \mathbf{A}_i(\widetilde{\boldsymbol{\theta}}))^{-1}\mathbf{B}_i(\widetilde{\boldsymbol{\theta}}) + \mathbf{D}_i(\widetilde{\boldsymbol{\theta}}) \\
\boldsymbol{\Upsilon}_i(p^{-1}, \widetilde{\boldsymbol{\theta}}) &= \mathbf{C}_i(\widetilde{\boldsymbol{\theta}})(p\mathbf{I} - \mathbf{A}_i(\widetilde{\boldsymbol{\theta}}))^{-1}\mathbf{F}_{xi}(\widetilde{\boldsymbol{\theta}}) + \mathbf{F}_{y_i}(\widetilde{\boldsymbol{\theta}}) \\
\mathbf{E}_{my_i}(p^{-1}, \widetilde{\boldsymbol{\theta}}) &= \mathbf{E}_{y_i}(\widetilde{\boldsymbol{\theta}})\frac{p}{p-1} \\
\mathbf{E}_{mxi}(p^{-1}, \widetilde{\boldsymbol{\theta}}) &= \mathbf{C}_i(\widetilde{\boldsymbol{\theta}})(p\mathbf{I} - \mathbf{A}_i(\widetilde{\boldsymbol{\theta}}))^{-1}\mathbf{E}_{xi}(\widetilde{\boldsymbol{\theta}})\frac{p}{p-1} \\
\mathbf{E}_{mi}(p^{-1}, \widetilde{\boldsymbol{\theta}}) &= \mathbf{E}_{my_i}(p^{-1}, (\widetilde{\boldsymbol{\theta}})) + \mathbf{E}_{mxi}(p^{-1}, \widetilde{\boldsymbol{\theta}}) \\
\boldsymbol{\Omega}_i(p^{-1}) &= \mathbf{N}_i
\end{aligned}$$

Table 1 summarizes when the transition function in HA is possibly defined. The symbol "$-$" indicates that the transition between the corresponding two modes is not possible. Notice that transitions between nominal modes are possible in any sense and transitions from faulty modes to nominal modes are not possible.

		Destination modes	
		$\mathcal{Q}_\mathcal{N}$	$\mathcal{Q}_\mathcal{F}$
Source modes	$\mathcal{Q}_\mathcal{N}$	$\Sigma_s \cup \Sigma_c$	$\Sigma_\mathcal{F}$
	$\mathcal{Q}_\mathcal{F}$	-	-

Table 1. Transition function defined for the HA

Another aspect to consider is that the composition of component automata is done for operation modes that belong to $\mathcal{Q}_\mathcal{N}$, whose dynamical behavior is described by equations (1)-(2). Faulty modes are added a posteriori to the resulting hybrid automaton. Thus, the number of faulty modes associated with each mode in $\mathcal{Q}_\mathcal{N}$ equals to $|\mathcal{F}|$. This model results from an adaptation of Lygeros et al. (2003); Bayoudh et al. (2008) and Vento et al. (2010).

2.2 *Overview of the proposed fault diagnosis approach*

Model-based FDI relies on comparing the estimated behavior of the system obtained from a non-faulty model with the real measured behavior available through sensor measurements (Cocquempot et al. 2004). The FDI algorithm for hybrid systems takes into account which is the current operation mode i of the hybrid system to adapt the model used to generate the predicted output. Thus, a set of residuals adapted to the mode dynamic behavior can be generated and evaluated as in the case of non-hybrid systems. The set of residuals for each mode including the uncertainty in parameters and noise is given by:

$$\mathbf{r}_i(k, \boldsymbol{\theta}) = \mathbf{y}(k) - (\widehat{\mathbf{y}}_i(k, \boldsymbol{\theta}) + \mathbf{N}_i\mathbf{n}(k)) \tag{4}$$

where $\mathbf{y}(k)$ is the real behavior and $\widehat{\mathbf{y}}_i(k, \boldsymbol{\theta})$ is estimated behavior considering parameter uncertainty $\boldsymbol{\theta} \in \left[\underline{\boldsymbol{\theta}}, \overline{\boldsymbol{\theta}}\right]$ in mode i. Additive noise $\mathbf{n}(k)$ bounded by the set $\mathcal{V}$ (i.e. $\mathbf{n}(k) \in \mathcal{V}$) represents the uncertainty about the exact knowledge of the real noise $\widetilde{\mathbf{n}}$. The predicted output can be obtained using observers or parity equations (Chow. and Willsky 1984; Blanke et al. 2006; Meseguer et al. 2010a).

The architecture to detect and isolate faults in hybrid systems is provided in Fig. 1. Two separate stages are considered for hybrid system diagnosis: offline and online processes. In the offline process, the hybrid automaton model is built through the component parallel composition and the generation of a set of equations which depend on the operation mode. Residuals for each mode are generated and an exploration of feasible hybrid automaton traces is carried out to study mode discernibility. Therefore, the discernibility study and observable events of the system allow to build a behavior automaton (B) (Vento et al. 2011). This information is used to predict which mode changes can be detected and isolated. Hence, a diagnoser is built from B applying the methodology developed by Sampath et al. (1995) for discrete-event systems diagnosis.

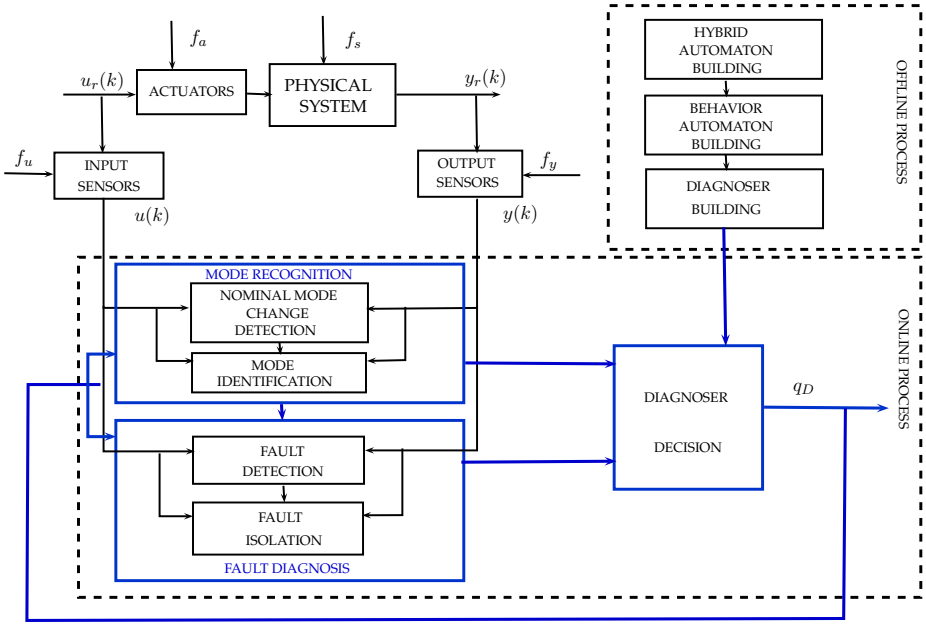

Figure 1. Conceptual block diagram for the hybrid system diagnosis methodology

On the other hand, in the online process, the tasks are carried out by the three blocks highlighted in blue in Fig. 1. *Mode recognition* and *fault diagnosis* blocks deal with possible changes in the system operation mode based on consistency indicators and observable event occurrences. Both blocks cooperate together. The *diagnoser decision* block gives a final diagnostic according to information provided by *mode recognition* and *fault diagnosis* blocks that takes into account the effect of model parameters and noise uncertainties, in residuals bounding their effect by zonotopes.

The current diagnoser state (q_D) contains information on all modes the system is possibly operating in. If more than one mode is contained in q_D, those modes are non discernible. A mode change in HA implies a nominal or a faulty mode change. In the online diagnosis, a set of events are identified describing a feasible trajectory of the physical system.

The discernibility property allows to predict wether a mode change can be detected and identified when the operation mode is described by a dynamic model (Bayoudh et al. 2008; Meseguer et al. 2010b; Cocquempot et al. 2004). In the case of faults, discernibility properties are related to *detectability* and *isolability* based on the fault signature matrix (Meseguer et al. 2010b) or based in the non-binarized sensitivity matrix (Blesa et al. 2012).

In online diagnosis, the following assumptions are made:

Assumption 1. *Two modes changes do not occur at the same time.*

Assumption 1 considers the fact that two events cannot be detected at the same time, since there would be uncertainty in the dynamic model to be used in the residual computation.

Assumption 2. *The residual dynamics have time to stabilize between two consecutive mode switchings.*

Assumption 2 implies that transitions between modes should be slower than the residual dynamics generator. This concerns the dwell time requirement, the time elapsed to reach the steady state in a stable way needed by the continuous dynamics of the operation modes before other transitions occur. Otherwise, the transition might not be correctly detected.

Assumption 3. *After a mode change occurrence, all the residuals sensitive to this change are activated at some time and persist during the whole mode change isolation process.*

Assumption 3 concerns the fact that the logic to detect and isolate mode changes is based on the steady state response of the set of residuals, assuming that the residuals sensitive to the mode change remain activated.

Assumption 4. *No mode change will occur after a fault has occurred.*

According to Assumption 4, once a fault has been detected, the online diagnosis process stops since it is assumed that the system does not further evolve. Whenever a fault occurs the set of residuals and models must be adapted to appropriately perform diagnosis. The considered faults affect the system parameters without changing the system configuration. This kind of faults leads to a loss of information, hence to compensate this the system model must be recalculated.

3. Fault detection

Consider the linear system represented by the state space model in discrete-time (1)-(2), the predicted output, using the parity space approach (Blanke et al. 2006), in matrix form is represented by:

$$\bar{\mathbf{Y}}(k) = \mathbf{O}_i(\boldsymbol{\theta})\mathbf{x}(k-\rho) + \mathbf{T}_{ui}(\boldsymbol{\theta})\bar{\mathbf{U}}(k) + \mathbf{T}_{f_i}(\boldsymbol{\theta})\bar{\mathbf{F}}(k) + \mathbf{T}_{Ei}(\boldsymbol{\theta}) + \mathbf{T}_{Ni}\bar{\mathbf{N}}(k) \tag{5}$$

where $\bar{\mathbf{Y}}(k) = \left[\mathbf{y}(k-\rho)\ \mathbf{y}(k-\rho+1)\cdots\mathbf{y}(k)\right]^T$ and $\bar{\mathbf{U}}(k) = \left[\mathbf{u}(k-\rho)\ \mathbf{u}(k-\rho+1)\cdots\mathbf{u}(k)\right]^T$ and $\bar{\mathbf{F}}(k) = \left[\mathbf{f}(k-\rho)\ \mathbf{f}(k-\rho+1)\cdots\mathbf{f}(k)\right]^T$, $\bar{\mathbf{N}}(k) = \left[\mathbf{n}(k-\rho)\ \mathbf{n}(k-\rho+1)\cdots\mathbf{n}(k)\right]^T$ and ρ is the parity space order. The parity space matrices are given by:

$$\mathbf{T}_{ui}(\boldsymbol{\theta}) = \begin{bmatrix} \mathbf{D}_i(\boldsymbol{\theta}) & \cdots 0 & 0 \\ \mathbf{C}_i(\boldsymbol{\theta})\mathbf{B}_i(\boldsymbol{\theta}) & \cdots 0 & 0 \\ \vdots & \ddots & \vdots \\ \mathbf{C}_i(\boldsymbol{\theta})(\mathbf{A}_i(\boldsymbol{\theta}))^{\rho-1}\mathbf{B}_i(\boldsymbol{\theta}) & \cdots & \mathbf{D}_i(\boldsymbol{\theta}) \end{bmatrix} \qquad \mathbf{T}_{Ni} = \begin{bmatrix} \mathbf{N}_i & \cdots 0 & 0 \\ 0 & \cdots 0 & 0 \\ \vdots & \ddots & \vdots \\ 0 & \cdots & \mathbf{N}_i \end{bmatrix}$$

$$\mathbf{T}_{Ei}(\boldsymbol{\theta}) = \begin{bmatrix} \mathbf{E}_{y_i}(\boldsymbol{\theta}) \\ \mathbf{C}_i(\boldsymbol{\theta})\mathbf{E}_{xi}(\boldsymbol{\theta}) + \mathbf{E}_{y_i}(\boldsymbol{\theta}) \\ \vdots \\ \mathbf{C}_i(\boldsymbol{\theta})(\mathbf{A}_i(\boldsymbol{\theta}))^{\rho-1}\mathbf{E}_{xi}(\boldsymbol{\theta}) + \cdots + \mathbf{E}_{y_i}(\boldsymbol{\theta}) \end{bmatrix} \qquad \mathbf{O}_i(\boldsymbol{\theta}) = \begin{bmatrix} \mathbf{C}_i(\boldsymbol{\theta}) \\ \mathbf{C}_i(\boldsymbol{\theta})\mathbf{A}_i(\boldsymbol{\theta}) \\ \vdots \\ \mathbf{C}_i(\boldsymbol{\theta})(\mathbf{A}_i(\boldsymbol{\theta}))^{\rho} \end{bmatrix}$$

$$\mathbf{T}_{f_i}(\boldsymbol{\theta}) = \begin{bmatrix} \mathbf{F}_{y_i}(\boldsymbol{\theta}) & \cdots 0 & 0 \\ \mathbf{C}_i(\boldsymbol{\theta})\mathbf{F}_{xi}(\boldsymbol{\theta}) & \cdots 0 & 0 \\ \vdots & \ddots & \vdots \\ \mathbf{C}_i(\boldsymbol{\theta})(\mathbf{A}_i(\boldsymbol{\theta}))^{\rho-1}\mathbf{F}_{xi}(\boldsymbol{\theta}) & \cdots & \mathbf{F}_{y_i}(\boldsymbol{\theta}) \end{bmatrix}$$

If there exists value of ρ such that

$$rank\left[\mathbf{O}_i(\boldsymbol{\theta})\ \mathbf{T}_{f_i}(\boldsymbol{\theta})\right] < (\rho+1)n_y \tag{6}$$

the left nullspace of $\left[\mathbf{O}_i(\boldsymbol{\theta})\ \mathbf{T}_{f_i}(\boldsymbol{\theta})\right]$ is not empty. The dimension of this subspace, n_r, is given as $n_r = (\rho+1)n_y - rank\left[\mathbf{O}_i(\boldsymbol{\theta})\ \mathbf{T}_{f_i}(\boldsymbol{\theta})\right]$. Condition (6) should be satisfied for all $\theta \in \Theta$. In Kołodziejczak (1999), a procedure to check the satisfaction of this condition is given based on testing a finite number of θ values.

Let $\mathbf{W}_i(\theta)$ be a $n_r \times (\rho+1)n_y$ matrix such that $\mathbf{W}_i(\theta)\mathbf{O}_i(\theta) = 0$. Multiplying the left and right terms of (5) by $\mathbf{W}_i(\theta)$ in such a way that eliminates the dependence of $\mathbf{x}(k)$, the analytical redundancy relations are expressed by the following equalities:

$$\mathbf{r}_i(k,\boldsymbol{\theta}) = \mathbf{W}_i(\boldsymbol{\theta})\bar{\mathbf{Y}}(k) - \mathbf{W}_i(\boldsymbol{\theta})\mathbf{T}_{ui}(\boldsymbol{\theta})\bar{\mathbf{U}}(k) - \mathbf{W}_i(\boldsymbol{\theta})\mathbf{T}_{Ei}(\boldsymbol{\theta}) - \mathbf{W}_i(\boldsymbol{\theta})\mathbf{T}_{Ni}\bar{\mathbf{N}}(k) = \mathbf{W}_i(\boldsymbol{\theta})\mathbf{T}_{f_i}(\boldsymbol{\theta})\bar{\mathbf{F}}(k) \tag{7}$$

Because of the inclusion of uncertain parameters in the continuous dynamics of the hybrid system model, the determination of $\mathbf{W}_i(\boldsymbol{\theta})$ is not a trivial task. One possible approach is proposed in Ploix and Adrot (2006). Here, a different approach, based on the equivalence that there exists between the parity space approach and input-output models (Ding et al. 2008), is used. Assume that the system model input-output form at a given operating point where the j^{th} output respect to the l^{th} input in mode i is described the following transfer function:

$$y^j(p,\boldsymbol{\theta}) = \frac{b_{\rho,i}(\boldsymbol{\theta})p^{\rho} + b_{\rho-1,i}(\boldsymbol{\theta})p^{\rho-1} + \cdots + b_{0,i}(\boldsymbol{\theta})}{p^{\rho} + a_{\rho-1,i}(\boldsymbol{\theta})p^{\rho-1} + \cdots + a_{0,i}(\boldsymbol{\theta})}u^l(p) \tag{8}$$

A way to construct the parity space residuals is based on defining the transformation vector as follows

$$\mathbf{W}_i(\boldsymbol{\theta}) = \left[a_{0,i}(\boldsymbol{\theta}) \cdots a_{\rho-1,i}(\boldsymbol{\theta})\ 1\right] \tag{9}$$

This definition can be justified according to the Cayley-Hamilton theorem. Following this theorem, it can be proved that $\mathbf{W}_i(\boldsymbol{\theta})\mathbf{O}_i(\boldsymbol{\theta}) = 0$ is satisfied by considering each output of Equation (8) independently:

$$A_i(\boldsymbol{\theta})^{\rho} + a_{\rho-1,i}(\boldsymbol{\theta})A_i(\boldsymbol{\theta})^{\rho-1} + \cdots + a_{0,i}(\boldsymbol{\theta})A_i(\boldsymbol{\theta}) = 0$$

$$\Rightarrow \begin{bmatrix} a_{0,i}(\boldsymbol{\theta}) \cdots a_{\rho-1,i}(\boldsymbol{\theta}) \ 1 \end{bmatrix} \begin{bmatrix} \mathbf{c}_i(\boldsymbol{\theta}) \\ \mathbf{c}_i(\boldsymbol{\theta})\mathbf{A}_i(\boldsymbol{\theta}) \\ \vdots \\ \mathbf{c}_i(\boldsymbol{\theta})\mathbf{A}_i(\boldsymbol{\theta})^{\rho} \end{bmatrix} = 0$$

where $\mathbf{A}_i(\boldsymbol{\theta}), \mathbf{c}_i(\boldsymbol{\theta})$ denotes the state space matrices of the transfer function given by Equation (8). Moreover,

$$\mathbf{W}_i(\boldsymbol{\theta})\mathbf{T}_{ui}(\boldsymbol{\theta}) = \begin{bmatrix} b_{0,i}(\boldsymbol{\theta}) \cdots b_{\rho-1,i}(\boldsymbol{\theta}) \ b_{\rho,i}(\boldsymbol{\theta}) \end{bmatrix}$$

$$\mathbf{W}_i(\boldsymbol{\theta})\mathbf{T}_{Ni} = \begin{bmatrix} a_{0,i}(\boldsymbol{\theta})\mathbf{N}_i \cdots a_{\rho-1,i}(\boldsymbol{\theta})\mathbf{N}_i \ \mathbf{N}_i \end{bmatrix}$$

and

$$\mathbf{W}_i(\boldsymbol{\theta})\mathbf{T}_{Ei}(\boldsymbol{\theta}) = \begin{bmatrix} e_{0,i}(\boldsymbol{\theta}) \cdots e_{\rho-1,i}(\boldsymbol{\theta}) \ e_{\rho,i}(\boldsymbol{\theta}) \end{bmatrix}$$

Under this approach, the number of residuals is equal to the number of system outputs for a given mode.

Alternatively, the residuals can be expressed using the input-output form according to Meseguer et al. (2010a) as follows:

$$\mathbf{r}_i(k,\boldsymbol{\theta}) = (\mathbf{I} - \mathbf{H}_i(p^{-1},\boldsymbol{\theta}))(\mathbf{y}(k) - \mathbf{N}_i\mathbf{n}(k)) - \mathbf{G}_i(p^{-1},\boldsymbol{\theta})\mathbf{u}(k) - \mathbf{E}_{mi}(p^{-1},\boldsymbol{\theta}) \tag{10}$$

where $\mathbf{G}_i(p^{-1},\boldsymbol{\theta})$, $\mathbf{H}_i(p^{-1},\boldsymbol{\theta})$ and $\mathbf{E}_{mi}(p^{-1},\boldsymbol{\theta})$ can be obtained from the input-output model in predictor form. Moreover, with the previous selection of $\mathbf{W}_i(\boldsymbol{\theta})$, an equivalence between input/ouput and parity space predictors can be established through the following relations:

$$\mathbf{H}_i(p^{-1},\boldsymbol{\theta})(\mathbf{y}(k) - \mathbf{N}_i\mathbf{n}(k)) = \mathbf{W}_i(\boldsymbol{\theta}) \begin{bmatrix} \mathbf{I}p^{-\rho} \\ \vdots \\ \mathbf{I} \end{bmatrix} (\mathbf{y}(k) - \mathbf{N}_i\mathbf{n}(k))$$

$$\mathbf{G}_i(p^{-1},\boldsymbol{\theta})\mathbf{u}(k) = \mathbf{W}_i(\boldsymbol{\theta})\mathbf{T}_{ui}(\boldsymbol{\theta})\mathbf{u}(k)$$

$$\mathbf{E}_{mi}(p^{-1},\boldsymbol{\theta}) = \mathbf{W}_i(\boldsymbol{\theta})\mathbf{T}_{Ei}(\boldsymbol{\theta})$$

3.1 *Parity space in regressor form*

From (7), a model in regressor form for every output can be obtained

$$y^j(k) = \psi_i^j(k)\xi_i + e_i^j(k) \ j = 1 \cdots n_y \tag{11}$$

where

- $\psi_i^j(k)$ is the regressor vector of dimension $1 \times n_{\xi,i}$ which can contain any function of inputs $u(k)$ and outputs $y^j(k)$.
- $\xi_i \in \Xi_i$ is the parameter vector of dimension $n_{\xi,i} \times 1$
- Ξ_i is the set that bounds the parameter ξ_i values.
- $e_i^j(k)$ is the additive error bounded by a constant $|e_i^j(k)| \leq \varepsilon_i^j$.

Remark 3.1. The dependence of parameter vector ξ_i and additive error $e_i^j(k)$ in Eq. (11) with respect to the parameter vector $\boldsymbol{\theta}$ and additive error $n^j(k)$ in Eq. (2) can be analytically obtained from Eq. (7).

Remark 3.2. In the same way, set Ξ_i and bounds ε^j can be related to sets $\boldsymbol{\Theta}$ and $\mathcal{V}$.

The n_y individual models (11) in mode i can be expressed in a compact form as a *Multiple Input and Multiple Output* (MIMO) model

$$\mathbf{y}(k) = \boldsymbol{\Psi}_i(k)\xi_i + \boldsymbol{e}_i(k) \tag{12}$$

where

- $\boldsymbol{\Psi}_i(k)$ is the regressor matrix of dimension $n_y \times n_{\xi,i}$ that contains the regressor vectors.
- $\boldsymbol{e}_i(k)$ is a vector of dimension $n_y \times 1$ that contains the additive errors (including noise).

3.2 *Residual evaluation*

Considering that the parameter vector ξ_i is bounded by an interval set. *i.e*

$$\Xi_i = \left\{ \xi_i \in \Re^{n_{\xi,i}} | \underline{\xi}_i^j \leq \xi_i^j \leq \bar{\xi}_i^j \; j = 1, ..., n_{\xi,i} \right\} \tag{13}$$

that can be parametrized as a particular case of a zonotope (Blesa et al. 2011) as follows

$$\Xi_i = \xi_i^0 \oplus \mathbf{K}_i \mathbb{B}^{n_{\xi,i}} = \left\{ \xi_i^0 + \mathbf{K}_i z : z \in \mathbb{B}^{n_{\xi,i}} \right\} \tag{14}$$

with centre ξ_i^0 and matrix uncertainty shape $\mathbf{K}_i$ equal to a $n_{\xi,i} \times n_{\xi,i}$ diagonal matrix:

$$\xi_i^0 = \left(\frac{\underline{\xi}_i^1 + \bar{\xi}_i^1}{2}, \frac{\underline{\xi}_i^2 + \bar{\xi}_i^2}{2}, \cdots, \frac{\underline{\xi}_i^{n_{\xi,i}} + \bar{\xi}_i^{n_{\xi,i}}}{2} \right) \tag{15}$$

$$\mathbf{K}_i = diag \left(\frac{-\underline{\xi}_i^1 + \bar{\xi}_i^1}{2}, \frac{-\underline{\xi}_i^2 + \bar{\xi}_i^2}{2}, \cdots, \frac{-\underline{\xi}_i^{n_{\xi,i}} + \bar{\xi}_i^{n_{\xi,i}}}{2} \right) \tag{16}$$

and $\oplus$ denotes the Minkowski sum, $\mathbb{B}^{n_{\xi,i}} \in \Re^{n_{\xi,i} \times 1}$ is a unitary box composed by $n_{\xi,i}$ unitary ($\mathbb{B} = [-1, 1]$) interval vectors.

Considering model (12) residual (7) can be computed as

$$\mathbf{r}_i(k) = \mathbf{y}(k) - \boldsymbol{\Psi}_i(k)\xi_i - \boldsymbol{e}(k) \tag{17}$$

and taking into account uncertainty in parameters and in additive error, the residual can be bounded by a zonotope (Blesa et al. 2012) defined by

$$\mathbf{\Gamma}_i(k) = \left(\mathbf{y}(k) - \mathbf{\Psi}_i(k)\xi_i^0\right) \oplus \left(\mathbf{\Psi}_i(k)\mathbf{K}_i \;\; \mathbf{\Pi}_i\right) \mathbb{B}^{n_{\xi,i}+n_y} \tag{18}$$

with

$$\mathbf{\Pi}_i = diag\left(\varepsilon_i^1, \cdots, \varepsilon_i^{n_y}\right) \tag{19}$$

Then, an output measurement vector $\mathbf{y}(k)$ will be consistent with the model (12) if

$$\mathbf{0} \in \mathbf{\Gamma}_i(k) \tag{20}$$

where $\mathbf{0}$ is a vector of n_y zeros. Test (20) can be rewritten as

$$\mathbf{r}_i^0(k) \in \bar{\mathbf{\Gamma}}_i(k) \tag{21}$$

with $\mathbf{r}_i^0(k)$ the nominal residual

$$\mathbf{r}_i^0(k) = \mathbf{y}(k) - \mathbf{\Psi}_i(k)\xi_i^0 \tag{22}$$

and $\bar{\mathbf{\Gamma}}_i(k)$ the zonope with the same shape as $\mathbf{\Gamma}_i(k)$ but centered in zero

$$\bar{\mathbf{\Gamma}}_i(k) = \mathbf{0} \oplus \left(\mathbf{\Psi}_i(k)\mathbf{K}_i \;\; \mathbf{\Pi}_i\right) \mathbb{B}^{n_{\xi,i}+n_y} \tag{23}$$

Test (21) involves checking whether or not the nominal residual $\mathbf{r}_i^0(k)$ (point) belongs to the zonotope $\bar{\mathbf{\Gamma}}_i(k)$ (set) and can be implemented using Algorithm (1) that **consists in determining the feasibility of a linear constraint satisfaction problem that can be efficiently solved using linear programming (see Blesa et al. (2012))**.

Algorithm 1 IsConsistent($\mathbf{r}_i^0(k), \bar{\mathbf{\Gamma}}_i(k)$)

Require: $\mathbf{\Psi}_i(k), \mathbf{K}_i, \mathbf{\Pi}_i$

1: **if** $\exists z(k) \in \mathbb{B}^{n_{\xi,i}}$ and $\exists e_i^j(k) \in [-\varepsilon_i^j, \varepsilon_i^j], \forall j := 1, ..., n_y$ such that $r_i^{0,j} := \Psi_i^j(k)\mathbf{K}_i z(k) + e_i^j(k), \forall j := 1, ..., n_y$ **then**
2: **return true**
3: **else**
4: **return false**
5: **end if**

4. Fault isolation

The isolation module is responsible of identifying which is the fault that is present in the system. Faults are isolated by checking the observed fault signature with the fault signatures stored in the theoretical fault signature matrix.

For faults, the residual fault sensitivity can be determined using its internal form. In the case of the parity space approach, this form is given by (7) as follows:

$$\mathbf{r}_i(k) = \mathbf{W}_i(\boldsymbol{\theta})\mathbf{T}_{f_i}(\boldsymbol{\theta})\bar{\mathbf{F}}(k) \tag{24}$$

According to Meseguer et al. (2010a), the residual fault sensitivity is given by

$$\boldsymbol{\Lambda}_i(p^{-1}) = \frac{\partial \mathbf{r}_i(k)}{\partial \mathbf{f}} \tag{25}$$

Thus, the residual fault sensitivity under the parity space approach is given by:

$$\boldsymbol{\Lambda}_i(p^{-1}, \boldsymbol{\theta}) = \mathbf{W}_i(\boldsymbol{\theta})\mathbf{T}_{f_i}(\boldsymbol{\theta}) \begin{bmatrix} \mathbf{I}_{n_f} p^{-\rho} \\ \vdots \\ \mathbf{I}_{n_f} \end{bmatrix} \tag{26}$$

Remark 4.1. A set of n_f faults would be isolable by means of the sensitivity matrix $\Lambda_i(p^{-1}, \boldsymbol{\theta})$ if this matrix satisfies that $column\, rank(\Lambda_i(p^{-1}, \boldsymbol{\theta})) = n_f$ for all $\theta \in \Theta$. As previously indicated, in Kołodziejczak (1999), a procedure to check the satisfaction of this condition for all θ is given based on testing a finite number of θ values.

Defining $\boldsymbol{\Lambda}_i^0$ as

$$\boldsymbol{\Lambda}_i^0 = \boldsymbol{\Lambda}_i(p^{-1}, \boldsymbol{\theta}^0) \tag{27}$$

where $\boldsymbol{\theta}^0$ is the nominal parameter and considering single faults, the fault isolation procedure can be implemented by solving the following algorithm for $k \geq k_f$ as proposed in Blesa et al. (2012)

Algorithm 2 f_ι=Fault_Isolation($\mathbf{r}_i^0(k), \boldsymbol{\Lambda}_i^0$)

1: **for all** $j := 1, ..., n_f$ **do**

2: $\left(J_{i,j}^{opt}(k), f_{i,j}^{opt}(k)\right) := \min_f J_{i,j}(f, k)$

subject to $J_{i,j}(f, k) := \sum_{h:=\max\{k_{fault}, k-\ell+1\}}^{k} \left\| r_i\left(h, \theta^0\right) - \lambda_{i,j}^0 f \right\|^2$

where $\lambda_{i,j}^0 := \partial r_i / \partial f_j$ is the j^{th} column of $\boldsymbol{\Lambda}_i^0$ and ℓ is the maximum time horizon

3: **end for**

4: $f_\iota := \arg \min_{j \in \{1, \cdots, n_f\}} \left\{ J_{i,j}^{opt}(k) \right\}$

5: **return** f_ι

Remark 4.2. Algorithm 2 involves solving n_f multi-output least square error optimization problems in time horizon h for every n_f possible single faults. The most probable fault f_ι is determined as the fault that gives the minimum function cost $J_{i,j}(f, k)$ after solving the set of least square error problems for the set of considered single faults.

5. Mode recognition

The mode recognition task is implemented through the mode change detection and recognition modules (see Fig, 1).

5.0.1 *Mode change detection*

The aim of this module is to detect when a mode transition occurs in the hybrid system. The mode change detection from mode i to mode j is inferred when an inconsistency in the set of residuals of the mode i is detected while at the same time the set of residuals corresponding to mode j are proved to be consistent.

Definition 5.1. Two modes q_i and q_j are said to be weakly non-discernible if and only if residuals $\mathbf{r}_i^0(k)$ (generated considering the mode i model) and $\mathbf{r}_j^0(k)$ (generated considering the mode j model) both belonging to their zonotopic sets (i.e., $\mathbf{r}_i^0(k) \in \bar{\mathbf{\Gamma}}_i(k)$, $\mathbf{r}_j^0(k) \in \bar{\mathbf{\Gamma}}_j(k)$ holds) when they are computed using signals $(\mathbf{y}(k), \mathbf{u}(k))$ corresponding to mode q_i or mode q_j.

The notion of non-discernability was first introduced by Cocquempot et al. (2004), where necessary and sufficient conditions were provided for the parity space approach in the state space representation.

In the case that residuals are generated using the parity space approach, the discernibility function is equivalent to evaluate the following condition (deduced by Cocquempot et al. (2004)) without parametric uncertainty:

$$rank[\mathbf{O}_i] \neq rank[\mathbf{O}_j] \neq rank\left[\mathbf{O}_i\ \mathbf{O}_j\ \Delta_{ij}\right] \tag{28}$$

where $\Delta_{ij} = \mathbf{T}_{ui} - \mathbf{T}_{uj}$.

This condition can be extended considering parametric uncertainty and matrices $\mathbf{E}_{xi}$ and $\mathbf{E}_{y_i}$ appearing in the continuous dynamics of the hybrid model, such that proceeding with a similar analysis the condition of non discernibility can be rewritten as follows

$$rank[\mathbf{O}_i(\boldsymbol{\theta})] = rank[\mathbf{O}_j(\boldsymbol{\theta})] = rank\left[\mathbf{O}_i(\boldsymbol{\theta})\ \mathbf{O}_j(\boldsymbol{\theta})\ \Delta_{ij}(\boldsymbol{\theta})\ \Delta_{E_{ij}}(\boldsymbol{\theta})\right] \tag{29}$$

where $\Delta_{ij}(\boldsymbol{\theta}) = \mathbf{T}_{ui}(\boldsymbol{\theta}) - \mathbf{T}_{uj}(\boldsymbol{\theta})$ and $\Delta_{E_{ij}}(\boldsymbol{\theta}) = \mathbf{T}_{Ei}(\boldsymbol{\theta}) - \mathbf{T}_{Ej}(\boldsymbol{\theta})$.

Condition (29) should be satisfied for all $\theta \in \Theta$. As previously indicated regarding Condition (6), in Kołodziejczak (1999), a procedure to check the satisfaction of this condition for all θ is given based on testing a finite number of θ values.

Thus, the following property can be defined:

Definition 5.2. A mode change from mode q_i to mode q_j is detectable at time instant k if and only if the nominal residual of mode i fulfills $\mathbf{r}_i^0(k) \notin \bar{\mathbf{\Gamma}}_i(k)$ and the nominal residual of mode j fulfills $\mathbf{r}_j^0(k) \in \bar{\mathbf{\Gamma}}_j(k)$

This definition implies that a mode change from mode i to mode j is detectable if mode i and mode j are discernable.

5.0.2 *Mode change isolation*

Once a mode transition has been detected, the new mode should be identified. To identify it, the nominal residual of each possible successor mode are checked to verify which of them belong to their zonotopic set using Algorithm 1.

Definition 5.3. Two mode changes, $i \to j$ and $i \to l$ are isolable if the following conditions are satisfied at any time instant k:

(1) Both mode changes are detectable
(2) In the case of a mode change $i \to j$ the residuals satisfy: $\mathbf{r}_i^0(k) \notin \bar{\mathbf{\Gamma}}_i(k)$, $\mathbf{r}_j^0(k) \in \bar{\mathbf{\Gamma}}_j(k)$ and $\mathbf{r}_l^0(k) \notin \bar{\mathbf{\Gamma}}_l(k)$

(3) In the case of a mode change $i \rightarrow l$ the residuals satisfy: $\mathbf{r}_i^0(k) \notin \bar{\mathbf{\Gamma}}_i(k)$, $\mathbf{r}_j^0(k) \notin \bar{\mathbf{\Gamma}}_j(k)$ and $\mathbf{r}_l^0(k) \in \bar{\mathbf{\Gamma}}_l(k)$.

6. Hybrid diagnoser

The diagnoser automaton is a finite state machine $D =< \mathcal{Q}_D, \Sigma_D, T_D, q_{D_0} >$, where:

- $q_{D_0} = \{q_0, \emptyset\}$ is the initial state of the diagnoser, which is assumed to correspond to a nominal system mode.
- $\mathcal{Q}_D$ is the set of the diagnoser states. An element $q_D \in \mathcal{Q}_D$ is a set of the form $q_D = \{(q_1, l_1), (q_2, l_2), \cdots (q_n, l_n)\}$, where $q_i \in \mathcal{Q}$ and $l_i \in \Delta$ where Δ defines the power set of fault labels with $\Delta_{\mathcal{F}} = \{f_1, \cdots, f_\gamma\}$, γ is the total number of faults in the system and $\gamma \in \mathcal{Z}^+$. In $\Delta_{\mathcal{F}}$, $\emptyset$ represents the nominal behavior,
- $\Sigma_D = \overline{\Sigma}_o$ is the set of all observable events.
- $\mathcal{T}_D : \mathcal{Q}_D \times \overline{\Sigma}_o \mapsto \mathcal{Q}_D$ is a partial transition function of the diagnoser.

The hybrid diagnoser is offline built following the methodology explained in Vento et al. (2011). The diagnoser performs diagnostics using online observations of the system behavior; it is also used to state and verify offline the necessary and sufficient conditions for diagnosability (Sampath et al. 1995). Faults are handled by discrete-event systems as unobservable events in the system model that are detected through the identified observable events. The diagnoser is represented by a finite state machine whose current state $q_{D_{current\_state}}$ contains the set of feasible modes the system is possibly operating in. The initial state is assumed to be known.

On the other hand, Algorithm 3 briefly describes the residual-based reasoning carried out by the diagnoser to identify an event occurrence. The algorithm checks for the current diagnoser state whether $\mathbf{r}^0_{current\_state}(k) \in \bar{\mathbf{\Gamma}}_{current\_state}(k)$ holds or not. In case of a diagnoser state change, by means of signature events, the set of residuals of some successor diagnoser state will fulfill $\mathbf{r}^0_{succ\_state}(k) \in \bar{\mathbf{\Gamma}}_{succ\_state}(k)$. In the case of a fault, the set of residuals in the current diagnoser state are compared with the sensitivity function as explained in Section 4 to isolate the fault. State successors are denoted by $Succs(q_{D_{current\_state}}) = \{q_{D_{succ\_state}} \in \mathcal{Q}_D : \exists \sigma \in \Sigma_D : \mathcal{T}_D(q_{D_{current\_state}}, \sigma) = q_{D_{succ\_state}}\}$. When observable events occur they are identified instantaneously (see line 8 in Algorithm 3).

7. Results

7.1 *Case Study Description*

The application case study is based on a part of the Barcelona sewer network. In general, sewers are pipelines that collect and transport wastewater from city buildings and rain drains to treatment facilities before being released to the sea. Sewers are generally gravity operated, though pumps may be used if necessary (Ocampo and Puig 2009).

The city of Barcelona has a combined sewer system (waste and rainwater go into the same sewer) of approximately 1500 Km. Additionally, the yearly rainfall is not very high (600 mm/year), but it includes storms typical of the Mediterranean climate that cause a lot of flooding problems and combined sewer overflows to the sea that cause pollution. Such a complex system is conducted through a control center in CLABSA (Barcelona Sewer Company) using a remote control system (in operation since 1994) that includes sensors, regulators, remote stations and communications. Nowadays, the urban drainage system contains 21 pumping stations, 36 gates, 10 valves and 10 retention tanks which are regulated in order to prevent flooding and combined sewer overflow to the environment. The remote control system is equipped with 56 remote stations including 22 rain-gauges and 136 water-level sensors which provide real-time information about rainfall and water level into the sewer system. All this information is centralized at the CLABSA Control Center through a supervisory control and data acquisition (SCADA) system.

Algorithm 3 Hybrid_Diagnoser

1: $current\_state := 0$
2: **loop**
3: $\urcorner(q_{D_{current\_state}}) := \{\sigma \in \Sigma_D : \mathcal{T}_D(q_{D_{current\_state}}, \sigma)$ is defined.$\}$
4: **while** IsConsistent($\mathbf{r}^0_{current\_state}(k), \bar{\mathbf{\Gamma}}_{current\_state}(k)$) **and** $\sigma_o \in \urcorner(q_{D_{current\_state}})$ does not occur **do**
5: Evaluate $\mathbf{r}^0_{current\_state}(k)$ according to (7)
6: **end while**
7: $next\_state := current\_state$
8: **if** σ_o occured **then**
9: $next\_state$ is such that $q_{D_{next\_state}} := \mathcal{T}_D(q_{D_{current\_state}}, \sigma_o)$
10: **print** `Transition from diagnoser state` $q_{D_{current\_state}}$ `to` $q_{D_{next\_state}}$
11: $current\_state := next\_state$
12: **else**
13: **for all** $q_{D_{succ\_state}} \in Succs(q_{D_{current\_state}})$ **do**
14: **if** IsConsistent($\mathbf{r}^0_{succ\_state}(k), \bar{\mathbf{\Gamma}}_{succ\_state}(k)$) **then**
15: **print** `Transition from diagnoser state` $q_{D_{current\_state}}$ `to` $q_{D_{succ\_state}}$
16: $current\_state := succ\_state$
17: **break**
18: **end if**
19: **end for**
20: **if** $next\_state = current\_state$ **then**
21: $f_\iota :=$ Fault_Isolation($\mathbf{r}^0_{current\_state}(k), \Lambda^0_{current\_state}$);
22: **print** `Fault` f_ι `has occurred`
23: **return**
24: **end if**
25: **end if**
26: **end loop**

There are two wastewater treatment plants (labeled with $WWTP1$ and $WWTP2$ in Fig. 2). A wastewater treatment plant consists in plants where, through physicochemical and biological processes, organic matter, bacteria, viruses and solids are removed from wastewaters before they are discharged in rivers, lakes and seas. Nowadays the inclusion of such elements within the sewer networks is of great significance in order to preserve the ecosystem and maintain the environmental balance inside the water cycle.

Fig. 2 shows the model of the considered part of the Barcelona network using the virtual tank modeling approach (Ocampo and Puig 2009). In order to illustrate the methodology, let us consider only tanks T_1, T_2 and T_3, placed inside the red square in Fig. 2.

The elements that appear in the considered part in Fig. 2 are: two virtual tanks (T_0, and T_1), one real tank (T_2), three limnimeters to measure the sewer levels (L_{39}, L_{41} and L_{47}), two rain gauges to measure the input rain intensity in the virtual tanks (P_{19} and P_{16}), and two redirection gates placed downstream T_0 and T_1, which allow to change the flow direction. In this particular case study, fixed position gates have been assumed.

The dynamic model of the virtual tank is given by the following discrete-time equation representing the water volume:

$$T_i : \qquad v_i(k+1) = v_i(k) + \Delta t(\varrho_i^{in}(k) - \varrho_i^{out}(k) - \varrho_i^{des}(k))$$

with $i \in \{0, 1\}$**. The overflow is given by:**

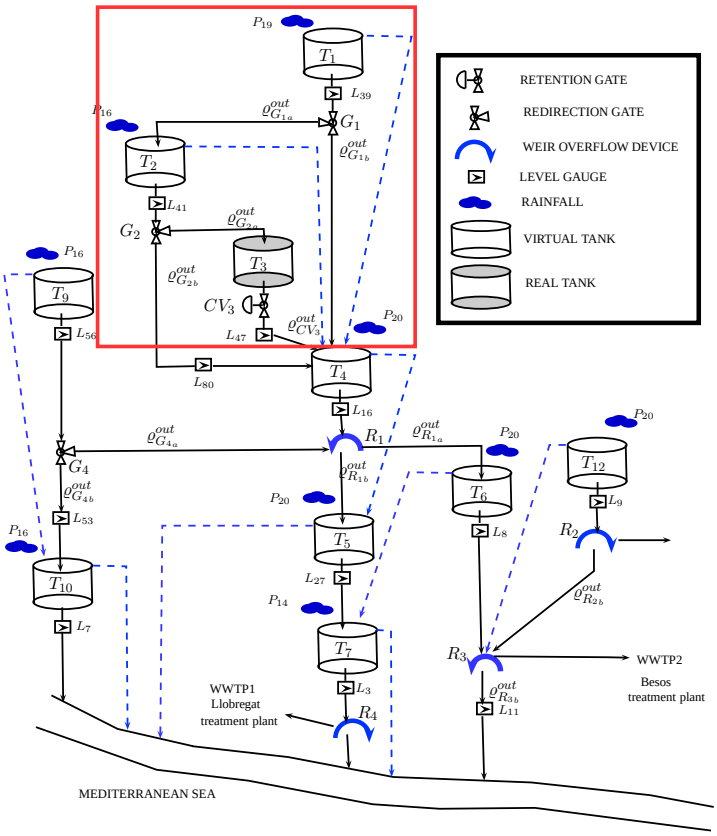

Figure 2. Barcelona test catchment

$$\varrho_i^{des}(k) = \begin{cases} \varrho_i^{in}(k) - \varrho_i^{out}(k) \text{ if } v_i(k) \geq \overline{v}_i \\ 0 \qquad\qquad\qquad\quad \text{otherwise} \end{cases} \tag{30}$$

The input flow associated with a virtual tank is given by:

$$\varrho_i^{in} = \varrho_i^{pluv}(k) + \sum_{h=1}^{H} \varrho_i^{out_h}(k) + \sum_{l=1}^{L} \varrho_i^{des_l}(k) \tag{31}$$

where $\varrho_i^{pluv}(k) = S_i \phi_i u_i(k)$ is associated with the rain intensity, $\varrho_i^{out_h}(k)$ corresponds to all the output flows of the other tanks pouring into tank T_i and $\varrho_i^{des_l}(k)$ corresponds to all overflows pouring into the tank T_i and $h, l \in \mathcal{Z}^+$.

The output flow for every tank is given by:

$$\varrho_i^{out}(k) = \begin{cases} \beta_i v_i(k) \text{ if } \varrho_i^{in}(k) < \varrho_i^{out}(k) \\ \beta_i \overline{v}_i \quad \text{if } v_i(k) \geq \overline{v}_i \end{cases} \tag{32}$$

The relation between level and volume and the measurements provided by the sensors are described by the equations below:

$$L_i(k) = \frac{\beta_i}{M_i} v_i(k) \tag{33}$$

The parameters of the sewer network are described in Table 2.

Parameter	description	units (MKS)
β_i	Volume to flow conversion factor of external tank T_i	$\frac{l}{s}$
M_i	Conversion factor in the output valve in T_i	-
S_i	Area of virtual tank T_i	m^2
γ_i	Absorption factor of tank T_i	-
$\overline{v_i}$	Maximum volume in tank T_i	m^3

Table 2. Virtual tank parameters

Hybrid phenomena like overflows in sewers and tanks (blue dash lines illustrate this overflow situation in Fig. 2, in virtual tanks) can appear and change their behavior. A hybrid model is used in order to describe such behavior and to design a hybrid diagnoser to detect and isolate faults. The Diagnoser reasons according to Algorithm 3, and it is built based on the methodology presented in Vento et al. (2011).

7.2 *Hybrid modeling*

The hybrid automata HA describing the sewer network is illustrated in Fig. 3. There are 24 operation modes which 4 of them are nominal operation modes (i.e., $|\mathcal{Q}_\mathcal{N}| = 4$) corresponding to the overflow or no overflow conditions of the virtual tanks. In the figure such conditions are represented by *O* and *WO*, respectively. For example, mode 1 means that no tank is in overflow situation, mode 2 means that only T_0 is in overflow, mode 3 means only T_1 is in overflow and mode 4 both in overflow. The initial mode corresponds to $q_0 = q_1$. Transitions are bound to spontaneous mode switching events (e.g., no input events are considered) which are represented in the figure as inequalities. Such events are unobservable since state variables (e.g., tank volumes) are not measured. The other 20 modes correspond to faulty modes (i.e., $|\mathcal{Q}_\mathcal{F}| = |\mathcal{Q}_\mathcal{N}| \cdot |\mathcal{F}| = 20$) representing additive faults in sensors.

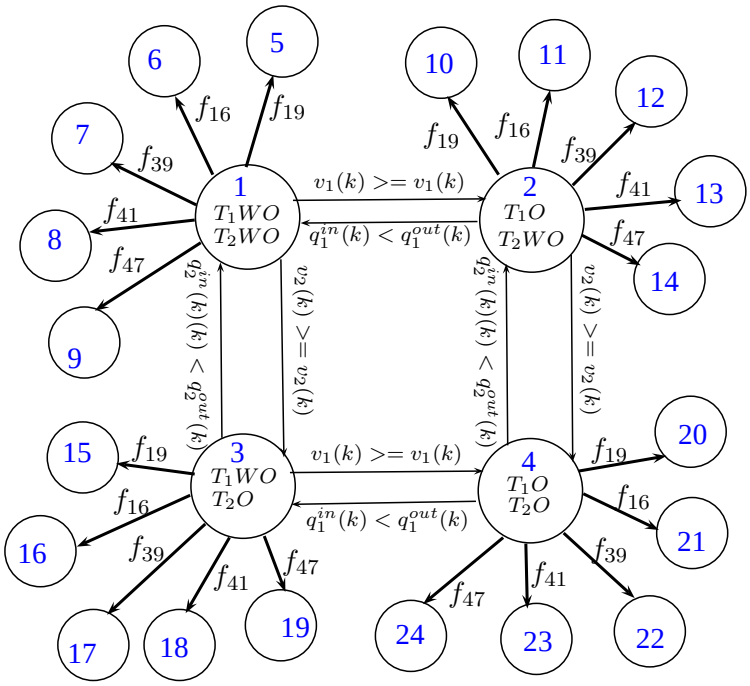

Figure 3. Hybrid automaton for the sewer network

For each mode, a different dynamical model according to hybrid model (1)-(2) is defined. The continuous dynamical model for each mode $q_i \in \mathcal{Q}_\mathcal{N} \cup \mathcal{Q}_{\mathcal{F}_s}$ is provided in Table 3.

q_i	$\mathbf{A}_i$	$\mathbf{B}_i$	$\mathbf{E}_{xi}$
1 $T_1, T_2 : WO$	$\begin{bmatrix} 1-\Delta t\beta_1 & 0 & 0 \\ \Delta t\beta_1 & 1-\Delta t\beta_2 & 0 \\ 0 & \Delta t\beta_2 & 1-\Delta t\beta_3 \end{bmatrix}$	$\begin{bmatrix} \Delta tS_1\varphi_{19} & 0 \\ 0 & \Delta tS_2\varphi_{16} \\ 0 & 0 \end{bmatrix}$	$\begin{bmatrix} 0 \\ 0 \\ 0 \end{bmatrix}$
2 $T_1 : O, T_2 : WO$	$\begin{bmatrix} 0 & 0 & 0 \\ 0 & 1-\Delta t\beta_2 & 0 \\ 0 & \Delta t\beta_2 & 1-\Delta t\beta_3 \end{bmatrix}$	$\begin{bmatrix} 0 & 0 \\ 0 & \Delta tS_2\varphi_{16} \\ 0 & 0 \end{bmatrix}$	$\begin{bmatrix} \overline{v_1} \\ \Delta t\beta_1\overline{v_1} \\ 0 \end{bmatrix}$
3 $T_1 : WO, T_2 : O$	$\begin{bmatrix} 1-\Delta t\beta_1 & 0 & 0 \\ 0 & 0 & 0 \\ 0 & 0 & 1-\Delta t\beta_3 \end{bmatrix}$	$\begin{bmatrix} \Delta tS_1\varphi_{19} & 0 \\ 0 & 0 \\ 0 & 0 \end{bmatrix}$	$\begin{bmatrix} 0 \\ \overline{v_2} \\ \Delta t\beta_2\overline{v_2} \end{bmatrix}$
4 $T_1, T_2 : O$	$\begin{bmatrix} 0 & 0 & 0 \\ 0 & 0 & 0 \\ 0 & 0 & \Delta t\beta_3 \end{bmatrix}$	$\begin{bmatrix} 0 & 0 \\ 0 & 0 \\ 0 & 0 \end{bmatrix}$	$\begin{bmatrix} \overline{v_1} \\ \overline{v_2} \\ \Delta t\beta_2\overline{v_2} \end{bmatrix}$

Table 3. **State space matrices for each mode $q_i \in \mathcal{Q}_\mathcal{N}$ where the tank volumes are the state variables**

The output function is given by equation (34)

$$\begin{bmatrix} y_1(k) \\ y_2(k) \\ y_3(k) \end{bmatrix} = \begin{bmatrix} \frac{\beta_1}{M_{39}} & 0 & 0 \\ 0 & \frac{\beta_2}{M_{41}} & 0 \\ 0 & 0 & \frac{\beta_3}{M_{47}} \end{bmatrix} \begin{bmatrix} x_1(k) \\ x_2(k) \\ x_3(k) \end{bmatrix} \tag{34}$$

with the same matrix $\mathbf{C}_i$ for all modes and $\mathbf{D}_i = \mathbf{0}$.

These continuous dynamical models have been used for residual generation. For instance, the predictor used for residual generation corresponding to all modes are detailed in Table 4.

q_i	$\mathbf{H}_i(\boldsymbol{\theta})$	$\mathbf{G}_i(\boldsymbol{\theta})$	$\mathbf{E}_{mi}(\boldsymbol{\theta})$	parameter uncertainty
1	$\begin{bmatrix} \theta_1 & 0 & 0 \\ \theta_2 & \theta_3 & 0 \\ 0 & \theta_4 & \theta_5 \end{bmatrix}$	$\begin{bmatrix} \theta_6 & 0 \\ 0 & \theta_7 \\ 0 & 0 \end{bmatrix}$	$\begin{bmatrix} 0 \\ 0 \\ 0 \end{bmatrix}$	$\theta_1 \in [0.7240, 0.8500]$ $\theta_5 \in [0.8648, 1.0152]$ $\theta_2 \in [0.1522, 0.1787]$ $\theta_6 \in [1.0388 \cdot 10^4, 1.2195 \cdot 10^4]$ $\theta_3 \in [0.7599, 0.8921]$ $\theta_7 \in [0.8648 \cdot 10^4, 4.8724 \cdot 10^4]$ $\theta_4 \in [0.0234, 0.0381]$
2	$\begin{bmatrix} 0 & 0 & 0 \\ 0 & \theta_1 & 0 \\ 0 & \theta_2 & \theta_3 \end{bmatrix}$	$\begin{bmatrix} 0 & 0 \\ 0 & \theta_4 \\ 0 & 0 \end{bmatrix}$	$\begin{bmatrix} \theta_5 \\ \theta_6 \\ 0 \end{bmatrix}$	$\theta_1 \in [0.7599, 0.8921]$ $\theta_4 \in [4.1506 \cdot 10^4, 4.1506 \cdot 10^4]$ $\theta_2 \in [0.0324, 0.0381]$ $\theta_5 \in [1.3848, 1.6257]$ $\theta_3 \in [0.8648, 1.0152]$ $\theta_6 \in [0.7390, 0.8676]$
3	$\begin{bmatrix} \theta_1 & 0 & 0 \\ 0 & 0 & 0 \\ 0 & 0 & \theta_2 \end{bmatrix}$	$\begin{bmatrix} \theta_3 & 0 \\ 0 & 0 \\ 0 & 0 \end{bmatrix}$	$\begin{bmatrix} 0 \\ \theta_4 \\ \theta_5 \end{bmatrix}$	$\theta_1 \in [0.7240, 0.8500]$ $\theta_4 \in [3.4697, 4.0731]$ $\theta_2 \in [0.8648, 1.0152]$ $\theta_5 \in [0.1222, 0.1435]$ $\theta_3 \in [1.0388 \cdot 10^4, 1.2195 \cdot 10^4]$
4	$\begin{bmatrix} 0 & 0 & 0 \\ 0 & 0 & 0 \\ 0 & 0 & \theta_1 \end{bmatrix}$	$\begin{bmatrix} 0 & 0 \\ 0 & 0 \\ 0 & 0 \end{bmatrix}$	$\begin{bmatrix} \theta_2 \\ \theta_3 \\ \theta_4 \end{bmatrix}$	$\theta_1 \in [0.8648, 1.0152]$ $\theta_3 \in [3.4697, 4.0731]$ $\theta_2 \in [1.3848, 1.6257]$ $\theta_4 \in [0.1222, 0.1435]$

Table 4. Residuals generation for $q_i \in \mathcal{Q}_\mathcal{N} \cup \mathcal{Q}_\mathcal{F}$

The uncertain parameters have been estimated using the algorithm proposed by Ploix and Adrot (2006) leading to the intervals shown in the last column. Since a different model corresponds to in each mode, the number of parameters also changes for each mode.

The residual expression for the sewer network can be expressed using the relation between parity space and predictor as follows:

$$\mathbf{r}_i(k) = \left[\mathbf{H}_i(\boldsymbol{\theta})\ \mathbf{I}\right] \left(\bar{\mathbf{Y}}(k) - \mathbf{N}_i\bar{\mathbf{N}}(k)\right) - \left[\mathbf{G}_i(\boldsymbol{\theta})\ \ \mathbf{0}\right] \bar{\mathbf{U}}(k) - \mathbf{E}_{mi}(\boldsymbol{\theta})$$

where the value of $\mathbf{W}_i(\boldsymbol{\theta})$ is given by:

$$\mathbf{W}_i(\boldsymbol{\theta}) = \left[\mathbf{H}_i(\boldsymbol{\theta})\ \mathbf{I}\right]$$

The additive error is bounded by $e_i^j = 0.1$. The fault set $\mathcal{F}$ includes faults in the output sensors (f_{L39}, f_{L41} and f_{L47}) as well as faults in the input sensors (f_{P19} and f_{P16}). Applying (26), the theoretical fault signature matrix is obtained selecting $\mathbf{F}_{y_i} = \left[\mathbf{0}\ \mathbf{I}\right]$ and $\mathbf{F}_{xi} = \left[-\mathbf{B}_i(\boldsymbol{\theta})\ \mathbf{0}\right]$ to represent output and input sensor faults respectively. The residual fault sensitivity matrices for each mode is given in Table 5.

$\boldsymbol{\Lambda}_i^0 = \boldsymbol{\Lambda}_i(p^{-1}, \boldsymbol{\theta}^0)$
$\begin{bmatrix} f_{P_{19}} & f_{P_{16}} & f_{L_{39}} & f_{L_{41}} & f_{L_{47}} \end{bmatrix}$
$\begin{bmatrix} -\frac{1.13\cdot10^4}{p} & 0 & 1.0-\frac{0.787}{p} & 0 & 0 \\ 0 & -\frac{4.51\cdot10^4}{p} & -\frac{0.165}{p} & 1.0-\frac{0.826}{p} & 0 \\ 0 & 0 & 0 & -\frac{0.0352}{p} & 1.0-\frac{0.94}{p} \end{bmatrix}$
$\begin{bmatrix} 0 & 0 & 1.0 & 0 & 0 \\ 0 & -\frac{4.51\cdot10^4}{p} & 0 & 1.0-\frac{0.826}{p} & 0 \\ 0 & 0 & 0 & -\frac{0.0352}{p} & 1.0-\frac{0.94}{p} \end{bmatrix}$
$\begin{bmatrix} -\frac{1.13\cdot10^4}{p} & 0 & 1.0-\frac{0.787}{p} & 0 & 0 \\ 0 & 0 & 0 & 1.0 & 0 \\ 0 & 0 & 0 & 0 & 1.0-\frac{0.94}{p} \end{bmatrix}$
$\begin{bmatrix} 0 & 0 & 1.0 & 0 & 0 \\ 0 & 0 & 0 & 1.0 & 0 \\ 0 & 0 & 0 & 0 & 1.0-\frac{0.94}{p} \end{bmatrix}$

Table 5. Sensitivity matrix for each mode q_i

These matrixes comprise five columns. The first and second ones correspond to input sensor faults, and the last three ones correspond to the output sensor faults. **Every column of the FS$_i$ is associated to a faulty mode in Fig. 3. For every nominal mode there are 4 faulty modes labeled from 9-24.**

The set $\Sigma_s = \{\sigma_{uo1}, \sigma_{uo2}, \sigma_{uo3}, \sigma_{uo4}\}$ represents the unobservable spontaneous events. Event σ_{uo1} corresponds to the volume in tank T_1 reaching its maximum, i.e. $v_1 \geq \overline{v}_1$. Event σ_{uo2} corresponds to the case in which the input flow is less than the output flow from T_1, i.e., $q_1^{in} < q_1^{out}$. The other events are related to the other virtual tanks. The set $\Sigma_{\mathcal{F}_{ns}} = \{\sigma_{f19}, \sigma_{f16}, \sigma_{f39}, \sigma_{f41}, \sigma_{f41}\}$ comprises the fault events related to faulty modes (in this case they correspond to sensor faults).

7.3 *Simulation scenarios*

The simulator of the sewer network implemented by Ocampo and Puig (2009) in Matlab, allows us to validate the methodology. Data provided by rain gauges corresponds to real episodes of rain occurred in Barcelona registered by CLABSA. The data provided by limnimeters is generated by the simulator through the rain gauge data.

A first simulation scenario (named as Scenario I in the following) illustrates the system state tracking and fault diagnosis. Fig. 4 shows the rain gauge measurements for the considered rain episode and the measurements provided by the limnimeters with a sample time of $\Delta t = 300s$. Therefore, the mode sequence can be deduced from system measurements.

Fig. 5 shows in solid line the simulated system state evolution for Scenario I, whereas the dash line is the state sequence estimated by the diagnoser.

The state sequence is $q_1 \rightarrow q_3 \rightarrow q_1 \rightarrow q_5$. Initially, neither virtual tank is in overflow. Next, T_1 is in overflow whereas later T_1 leaves the overflow condition. Finally, a fault in sensor P_{19} is simulated. Fig. 6 illustrates the residual evolution (nominal residual components $\mathbf{r}_i^0(k)$ (in green in the figure), bound

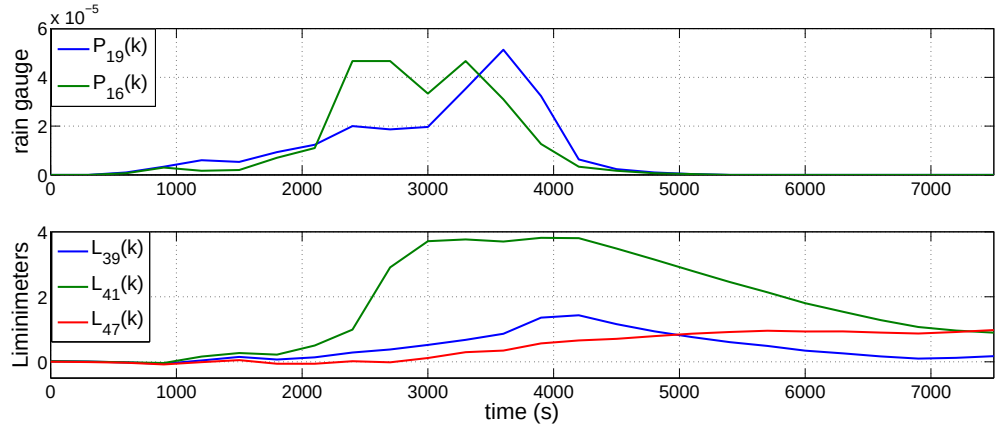

Figure 4. Example of a rain episode occurred in Barcelona

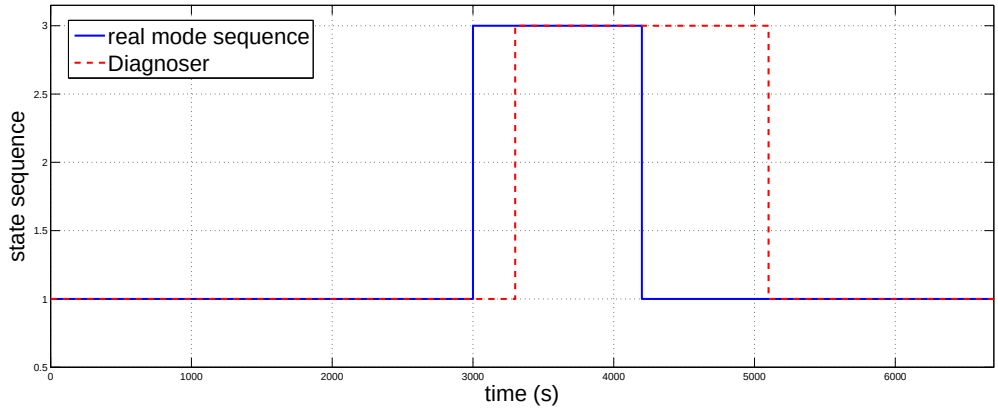

Figure 5. State diagnoser sequence vs mode sequence for Scenario I

projections of $\bar{\mathbf{\Gamma}}_i(k)$ (in blue and red in the figure) and **the incoming event occurrence correspond to the black vertical lines. The associated signature-events are detailed in Table 6**) for the considered scenario. Notice that, for instance, when a transition from mode $q_1 \rightarrow q_3$ occurs then $\mathbf{r}_1^0(k) \notin \bar{\mathbf{\Gamma}}_1(k)$ and $\mathbf{r}_3^0(k) \in \bar{\mathbf{\Gamma}}_3(k)$ holds. Notice that all modes are discernable according to the criterion explained in Section 5. Then, the fault is detected comparing the observed signature with the theoretical signature according to Section 4.

Consider the same scenario, but the set of residuals are binarized using fixed thresholds τ_i corresponding to the highest zonotopes bounds in order to avoid false alarms (see Fig. 7). In Fig 8, the corresponding diagnoser state sequence is shown. Notice that when using a fixed threshold, some mode changes may be detected later by the diagnoser (an extra delay appears in the mode detection process). Moreover, in the case of the fault in sensor P_{19}, the residual sensitive to the fault is activated later (after three samples) and oscillates inside and outside its threshold bounds. This complicates the detection process by the diagnoser.

Consider another scenario (named as Scenario II), where an additive fault in sensor L_{39} occurs at time $3600s$. Consequently the residuals of mode q_3 are triggered and the diagnoser stops. Notice that in Fig. 9, when the fault occurs $\mathbf{r}_3^0(k) \notin \bar{\mathbf{\Gamma}}_3(k)$ holds. Then, Algorithm 2 is activated and determines that the most probable fault is a fault in sensor L_{39}. In the case of using fixed thresholds, the results are similar sice the zonotope $\bar{\mathbf{\Gamma}}_3(k)$ bounds at this time instant are close to the maximum limit (threshold).

Fig. 10 shows in solid line the simulated system state evolution for Scenario II, whereas the dash line is the state sequence estimated by the diagnoser.

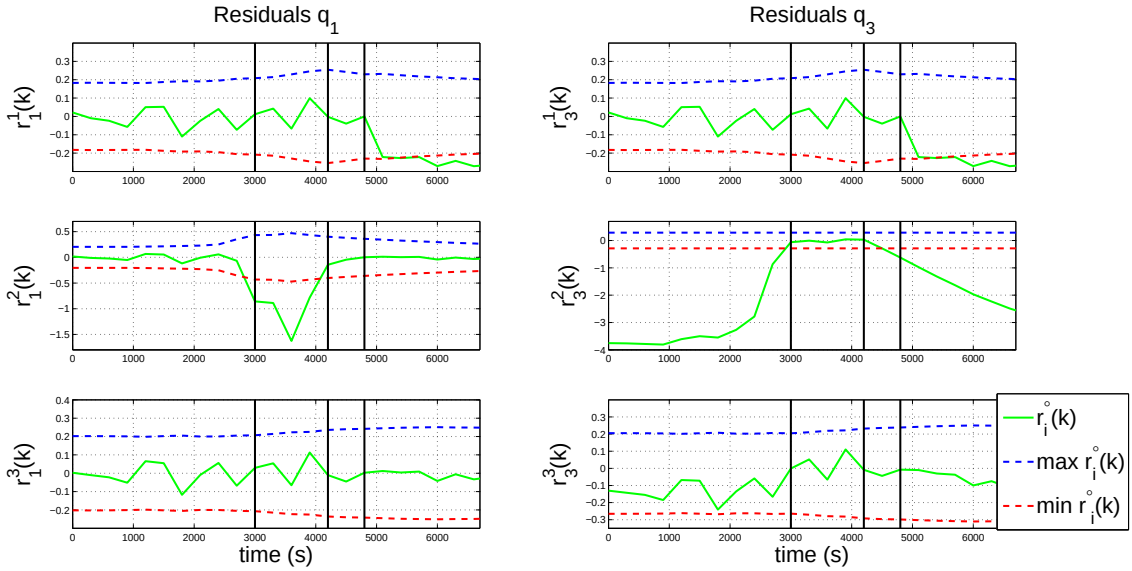

Figure 6. Mode change and fault detection using interval models for Scenario I

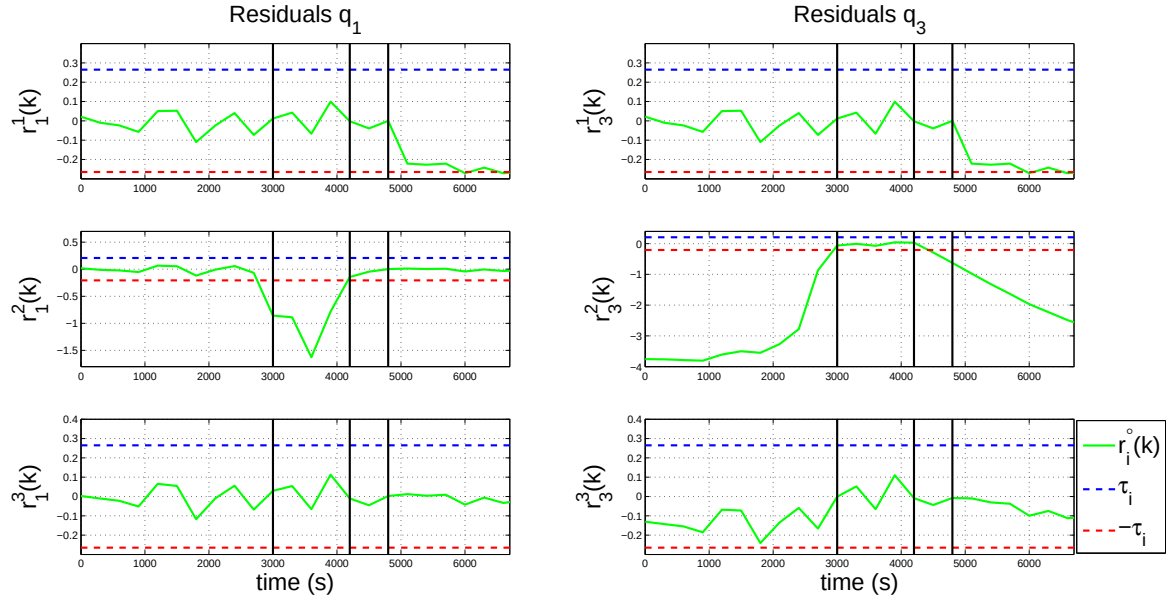

Figure 7. **Fault detection using a fixed threshold for Scenario I**

7.4 *Analysis*

The diagnoser report is provided in Table 6 for both scenarios. Transition $q_1 \rightarrow q_3$ occurs at $3000s$ and it is reported at $3300s$ and $q_1 \rightarrow q_3$ occurs at $4200s$ is reported at $5100s$. For Scenario II, an additive fault in sensor L_{39} appears at time $3600s$ and it is detected at $3900s$ when the system is in mode q_3. A delay is present since the residuals have a first order dynamic behavior and uncertainty is taken into account.

After detecting a fault, continuous dynamics must be recomputed to take into account the fault effect. Faults affect the continuous model used to generated the set of residuals. The loss of information should be compensated otherwise diagnosis would be erroneous (see Fig. 10). This is not a trivial task. It could be considered whenever a new system model have a reasonable online execution time to update it.

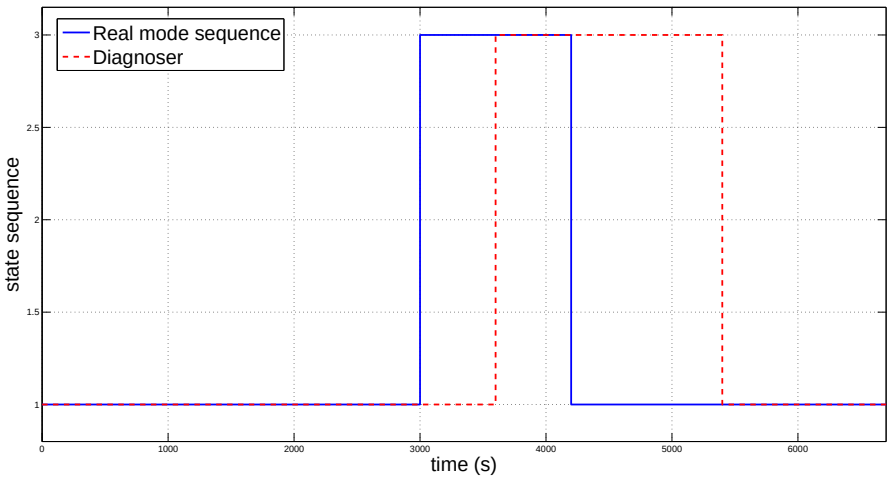

Figure 8. **State diagnoser sequence vs mode sequence for Scenario I using a fixed threshold**

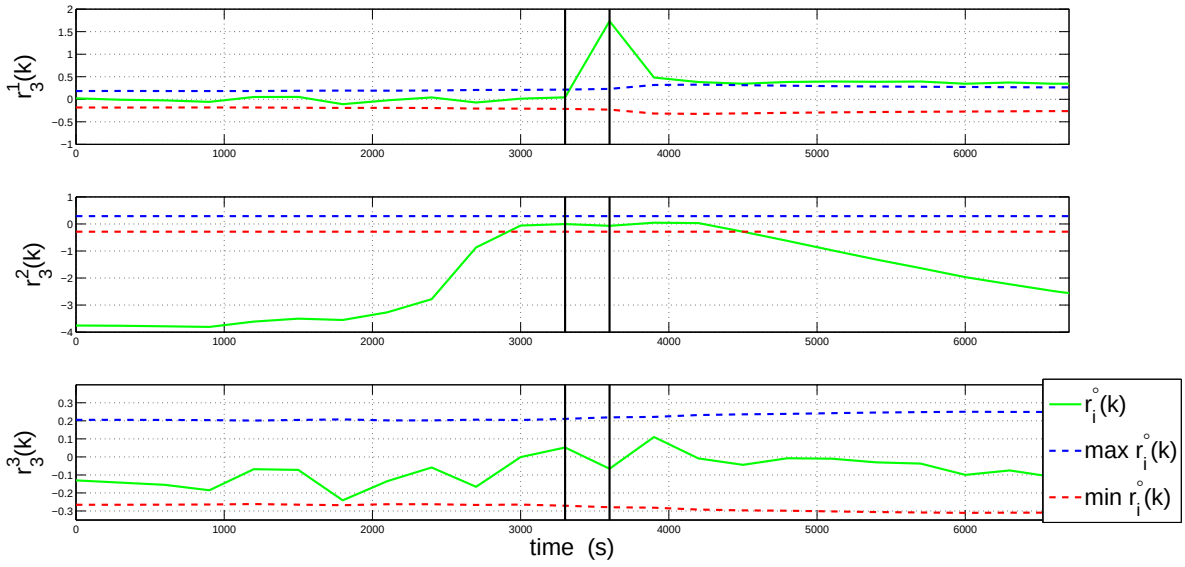

Figure 9. Fault detection using interval models for Scenario II

The occurrence time between two transitions in HA is an important aspect to be considered. The sampling time, the residuals dynamics and the observable events occurrence play an important role in hybrid diagnosis. For this reason, the methodology assumes that events can sequentially occur during the system evolution in a minimal time between them (see Assumption 2). This time is associated with the dwell time and the sampling time. As it can be seen in Table 6, whenever there is a mode change, the algorithms to compute residuals, verify consistency tests and update the current diagnoser state can be executed in realtime $(\leq 300s)$ for the sewer network.

The use of a binary coding would involve a loss of information since the residual activation might exhibit different dynamics (slow or fast). Zonotopes improve the fault detection algorithm, avoiding the loss of information. The sensitivity function without binarization allows a major degree of discernability between modes. Full mode discernibility is verified for the considered part of the sewer network.

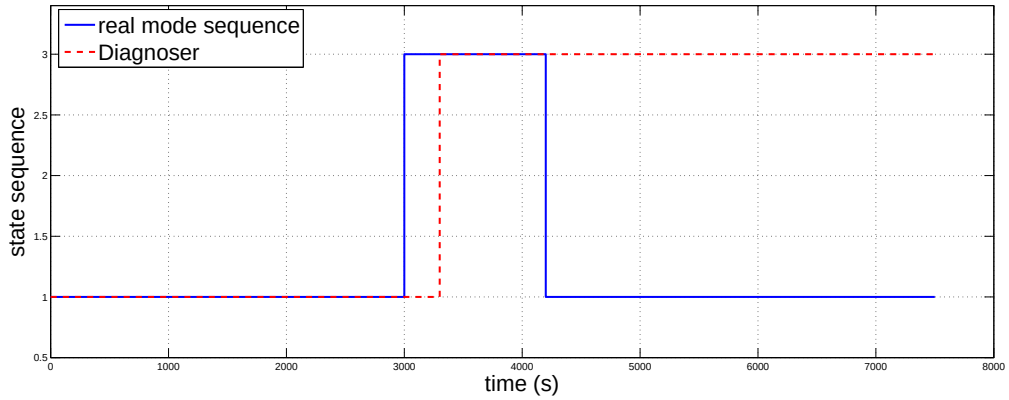

Figure 10. State diagnoser sequence vs mode sequence for Scenario II

Mode change	Reported event	State diagnoser	Occurrence time (s)	Detection time (s)	
				Adaptive threshold	Fixed threshold
Scenario I					
$q_1 \rightarrow q_3$	δ_{14}	$(q_3, \{\})$	3000	3300	3600
$q_3 \rightarrow q_1$	δ_{41}	$(q_1, \{\})$	4200	5100	5400
$q_1 \rightarrow q_5$ fault $f_{P19} \in \mathcal{F}$ in Mode q_1	δ_{f_1}	$(q_1, \{f_1\})$	4800	5100	6000
Scenario II					
$q_1 \rightarrow q_3$	δ_{14}	$(q_3, \{\})$	3000	3300	3300
$q_3 \rightarrow q_{17}$ fault $f_{L39} \in \mathcal{F}$ in Mode q_3	δ_{f_3}	$(q_{17}, \{f_3\})$	3600	3900	3900

Table 6. Hybrid diagnoser report

8. Conclusions

In this paper, a methodology and architecture to design a diagnoser in the framework of hybrid systems considering uncertainty in the parameters and additive error has been proposed. The methodology is robust since it considers modeling errors in the parameters and additive errors that comprise the effects of noise in measurements and discretisation errors. The parity space equations are used to evaluate the residuals on-line eliminating the dependence of the state variables, and the uncertainty is determined based on the equivalence that there exists between input/output models and parity equations. Parity relations can be expressed in regressor form and an adaptive threshold that bounds the effect of model uncertainty in residuals can be generated using zonotopes. This allows to formulate the fault detection as a consistency test at every sampling time based on checking the non-existence of a parameter value in the parameter uncertainty set and additive error such that model in mode i is consistent with all the system measurements. The performance of the proposed approach has been successfully tested in a part of the Barcelona sewer network

Acknowledgements

This work has been funded by the Spanish Ministry of Science and Technology through the CICYT project WATMAN (ref. DPI2009-13744) and by the Spanish Ministry of Economy and Competitiveness through the CICYT project SHERECS (ref. DPI2011-26243) and EFFINET (Ref. FP7-ICT-2012-318556) of the European Commission.

References

Bayoudh, M., Travé-Massuyès, L., and Olive, X. (2008), "Hybrid Systems Diagnosis by Coupling Continuous and Discrete Event Techniques," in *Proceedings of the 17th International Federation of Automatic Control, World Congress, IFAC-WC*, Seoul (Korea), pp. 7265–7270.

Blanke, M., Kinnaert, M., Lunze, J., and Staroswiecki, M., *Diagnosis and Fault Tolerant Control*, 2nd ed., Springer (2006).

Blesa, J., Puig, V., and Saludes, J. (2011), "Identification for passive robust fault detection using zonotope-based set-membership approaches," *International Journal of Adaptive Control and Signal Processing*, 25(9), 788–812.

Blesa, J., Puig, V., and Saludes, J. (2012), "Robust identification and fault diagnosis based on uncertain multiple input-multiple output linear parameter varying parity equations and zonotopes," *Journal of Process Control*, 22(10), 1890 – 1912.

Bregon, A., Alonso, C., Biswas, G., Pulido, B., and Moya, N. (2010), "Hybrid Systems Fault Diagnosis with Possible conflicts," in *22nd International Workshop on Principles of Diagnosis*.

Chow., E., and Willsky, A. (1984), "Analytical Redundancy and the Design of Robust Failure Detection Systems," *IEEE Transactions on Automatic Control*, 29(7), 603–614.

Cocquempot, V., Mezyani, T., and Staroswiecki, M. (2004), "Fault Detection and Isolation for Hybrid Systems using Structured Parity Residuals," in *5th Asian Control Conference*.

Daigle, M. (2008), "A Qualitative Event-Based Approach to Fault Diagnosis of Hybrid Systems," Faculty of the Graduate School of Vanderbilt University, Nashville, Tennessee.

Ding, X., Kinnaert, M., Lunze, J., and Staroswiecki, M., *Model Based Fault Diagnosis Techniques*, Springer (2008).

Hofbaur, M., and Williams, B.C. (2004), "Hybrid Estimation of Complex Systems," *IEEE Transactions on Systems, Man, and Cybernetics - Part B: Cybernetics*, 34(5), 2178–2191.

, B. ans SzulcKołodziejczak, T. (1999), "Convex combinations of matrices Ů Full rank characterization," *Linear Algebra and its Applications*, 287(1), 215–222.

Lygeros, J., Henrik, K., and Zhang, J. (2003), "Dynamical Properties of Hybrid Automata," *IEEE Transactions on Automatic Control*, 48(1), 2–17.

Meseguer, J., Puig, V., and Escobet, T. (2010a), "Fault Diagnosis using a Timed Discrete Event Approach based on Interval Observers," *Systems, Man and Cybernetics, Part A: Systems and Humans, IEEE Transactions on*, 40(5), 900–916.

Meseguer, J., Puig, V., and Escobet, T. (2010b), "Observer gain effect in linear interval observer-based fault detection," *Journal of process control*, 20(8), 944–956.

Narasimhan, S., and Biswas, G. (2007), "Model-Based Diagnosis of Hybrid Systems," *IEEE Transactions on Systems, Man and Cybernetics*, 37(3).

Ocampo, C., and Puig, V. (2009), "Fault-tolerant model predictive control within the hybrid systems framework: Application to sewer networks," *International Journal of Adaptive Control and Signal Processing*, 23(8), 757–787.

Ploix, S., and Adrot, O. (2006), "Parity relations for linear uncertain dynamic systems," *Automatica*, 42, 1553–1562.

Sampath, M., Sengupta, R., and Lafortune, S. (1995), "Diagnosability of Discrete-Event System," *IEEE Transactions on Automatic Control*, 40(9), 1555–1575.

Travé-Massuyès, L., Bayoudh, M., and Olive, X. (2008), "Hybrid Systems Diagnosis by coupling Continuous and Discrete event Techniques," in *Proceedings of the 17th World Congress*, july, Seoul, Korea, pp. 7265–7270.

Vento, J., Puig, V., and Sarrate, R. (2010), "Fault Detection and Isolation of Hybrid System using Diagnosers that combine Discrete and Continuous Dynamics," in *Conference on Control and Fault Tolerant System*, october, Nice, France.

Vento, J., Puig, V., and Sarrate, R. (2011), "A Methodology for building a Fault Diagnoser for Hybrid Systems," in *9th European Workshop on Advance Control and Diagnosis*, November, Budapest, Hungary.

Vento, J., Puig, V., and Sarrate, R. (2012), "Parity Space Hybrid System Diagnosis under Model Uncertainty," in *20th Mediterranean Conference on Control and Automation (MED)*, July, Barcelona, Spain.